Journal of Alloys and Compounds, 185 (1992) 191–205
JALCOM 232

Permeability and diffusivity of hydrogen in palladium-rich Pd–Y(Gd)–Ag ternary alloys

Y. Sakamoto, F. L. Chen, M. Furukawa and M. Noguchi
Department of Materials Science and Engineering, Nagasaki University, Nagasaki 852 (Japan)

(Received September 6, 1991)

Abstract

The permeabilities and diffusivities of hydrogen in $Pd_{100-x-y}(Y(Gd))_xAg_y$ alloys, where $y=0$, 5, 10, 15, 20 and 24 at.% Ag and x (at.%) is the Y(Gd) content such that the condition $y+3x=24$ is satisfied, as possible diffusion membranes for hydrogen purification were measured at temperatures between 523 K and 673 K and input hydrogen pressures between 267 kPa and 667 kPa. From the permeabilities and diffusivities, the solubility constants in the alloys were calculated. The alloys $Pd_{95-x}(Y(Gd))_xAg_5$ with $x=6.3$ were the most permeable to hydrogen, and the permeability values were found to be about a factor of 2–2.5 higher than that in Pd–24at.%Ag alloy. The permeabilities are associated with the lattice expansion of the initial hydrogen-free alloys. Judging from the hardness measurements of the initial alloys, $Pd_{100-x-y}(Y(Gd))_xAg_y$ with compositions where y is about 15–20 at.% Ag, and x is about 1.3–3.0 at.% Y(Gd), seem to be better materials for hydrogen diffusion membranes than Pd–(23–25)at.%Ag alloys.

1. Introduction

It has been shown [1–4] that palladium-rich palladium–rare-earth (RE) solid solution alloys, especially alloys containing about 8 at.% yttrium, have superior permeability performance and could be used as possible diffusion membrane materials [5, 6] because they exhibit dimensional stability owing to suppression of the $(\alpha+\beta)$ hydrogen miscibility gaps [7, 8] during permeation, together with enhanced permeability compared with commercially available Pd–(23–25)at.%Ag alloys. The enhanced permeability in the Pd–8at.%Y alloy is associated with a steeper hydrogen solubility gradient at high temperatures.

However, there is significant solid solution hardening, together with greater lattice expansion in these Pd–RE binary alloys. On the one hand there is the possibility of producing a stronger membrane material, together with higher hydrogen permeability than in the plain Pd–Ag alloys, but on the other hand this extra hardening leads to problems in fabricating the material, which may be disadvantageous in practical applications of the alloys.

In a recent study of palladium-rich Pd–Y(Gd)–Ag ternary alloys [9] as possible diffusion membranes for hydrogen purification, it was shown that every one of the alloys $Pd_{100-x-y}(Y(Gd))_xAg_y$ with a silver content up to 24 at.% and content of yttrium and/or gadolinium x (at.%) together satisfying

0925-8388/92/$5.00

the condition $y+3x \leqq 24$, *i.e.* up to a valence electron concentration of $e/a=0.24$, forms a single α-Pd phase. However, electron diffraction and electrical resistance measurements on $Pd_{95-x}Gd_xAg_5$ with $x=6.3$ gave faint indications of short-range ordering of $Pd_7(Gd,Ag)$ type [10].

The lattice parameters a_{ss} of the hydrogen-free Pd–Y(Gd)–Ag alloys with a given silver content increase almost linearly with increasing yttrium and/or gadolinium content, and at the same composition the magnitude of the palladium lattice expansion upon gadolinium substitution is greater than that caused by the addition of yttrium [9]. Hardness measurements on ternary alloys with any given silver content showed that the hardnesses increase initially with increasing yttrium and/or gadolinium content and tend to have a plateau or inflection region around compositions where e/a is about 0.24.

The $(\alpha+\beta)$ hydrogen miscibility gaps at room temperature in hydrogenated Pd–Y(Gd)–Ag alloys with a given silver content decrease gradually with increasing yttrium and/or gadolinium content, and the critical compositions for the disappearance of the gaps are approximately isoelectronic with an electron-to-atom ratio such that $e/a=0.24$ [9]. The lattice parameters of the hydrogenated alloys at the critical compositions depend in each case on the magnitude of lattice expansion of the initial hydrogen-free alloys [11, 12].

Therefore, the alloys $Pd_{100-x-y}(Y(Gd))_xAg_y$ with compositions where $y=10$–20 at.% Ag and x (at.%) is the content of yttrium and/or gadolinium such that the condition $y+3x=24$ is approximately satisfied, seem to be better candidates for hydrogen diffusion membranes than the Pd–(23–25)at.%Ag employed commercially or Pd–8at.%Y binary alloy established by Hughes and Harris [2], because they are expected to have greater hydrogen permeability and to form stronger membranes than Pd–(23–25)at.%Ag, and to form softer membranes than Pd–8at.%Y.

The purpose of this study was to determine the permeability and diffusivity of hydrogen through the Pd–Y(Gd)–Ag alloys using pure hydrogen gas in the temperature and pressure ranges 523–673 K, and 267–667 kPa. The hydrogen permeability in the alloys is correlated with the lattice parameter and/or hardness of the initially hydrogen-free alloys.

2. Experimental details

2.1. Preparation of the samples

The alloys used in this study were prepared as before [9], and had compositions $Pd_{100-x-y}(Y(Gd))_xAg_y$, where $y=0$, 5, 10, 15, 20 and 24 at.% Ag, and x (at.%) is the content of yttrium and/or gadolinium such that condition $y+3x=24$ is satisfied, and at room temperature the hydrogen $(\alpha+\beta)$ miscibility gaps in the alloys are just closed at these compositions [9]. In addition to the alloys, the hydrogen permeability and diffusivity in pure palladium (purity 99.98 wt.%) were also measured for comparison.

All the disk samples 12 mm in diameter and 0.7 mm in thickness were cut from a cold rolled plate, and the surface was polished with a fine emery

paper. They were annealed at 1123 K for 2 h *in vacuo* and then furnace cooled to room temperature at a rate of 5–6 K min^{-1}. Prior to the permeation measurements, all the samples were chemically etched with a solution of 2:2:1 H_2SO_4:HNO_3:H_2O mixture in order to remove the oxide from the surface.

2.2. Apparatus and procedure

The apparatus for measuring the permeability and diffusivity of hydrogen is shown in Fig. 1, together with details of sample holder (Fig. 1(b)). Cajon 4VCR coupling made of 316 stainless steel was used for the sample holder and one of the glands was connected to a stainless steel bellows to provide the necessary flexibility. After mounting in the holder, both sides of the sample were evacuated to about 2×10^{-7} Torr, and simultaneously heated to the desired temperatures of 523, 573, 623 and 673 K respectively using a furnace. The sample temperature was maintained constant to within ±1 K and measured with a chromel–alumel thermocouple calibrated beforehand at the sample surface.

After evacuation the vacuum pump was isolated, and a recorder was started. A constant input hydrogen pressure $p_{H2,1}$ was applied to the sample, and an output pressure $p_{H2,2}$ was measured with an M.K.S. Baratron pressure gauge (G_2) as a function of time. The specified input hydrogen pressures $p_{H2,1}$ of 267, 400, 533 and 667 ± 2.7 kPa respectively were fixed by an M.K.S. pressure controller, working in conjunction with a control valve, and they were also monitored by the recorder through a pressure gauge (G_1). Before the next run at different pressures, the samples were again evacuated completely.

2.3. Mathematical basis of the permeability and diffusivity studies

Let us consider hydrogen permeation through the membrane as one-dimensional diffusion with diffusivity D independent of hydrogen concentration c. The hydrogen flow J_t per unit time which permeates a plane sample of area A and thickness L is measured [13, 14] by noting the pressure increase $p_{H2,2}$ in the output side whose volume V_2 has been calibrated. So that,

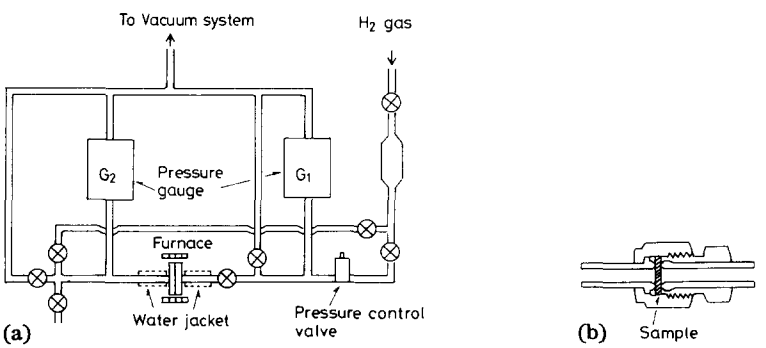

Fig. 1. Apparatus for hydrogen permeability measurement: (a) schematic diagram of the system, and (b) sample holder.

$$J_t = -D\left(\frac{\partial C}{\partial x}\right)_L = \frac{1}{A}\frac{dn_{H2}}{dt} = \frac{V_2}{ART_R}\frac{dp_{H2,2}}{dt} \quad (1)$$

where T_R is the temperature of the output side volume, V_2 and n_{H2} is the amount of permeated hydrogen gas.

The initial and boundary conditions are as follows: at $t=0$, $c=0$ for $0 \leqslant x \leqslant L$; at $t>0$, $c=c_1$ for $x=0$, and $c=c_2 \approx 0$ for $x=L$. Thus, the permeation rate J_t can be obtained [15] by solving the diffusion equation, $\partial c/\partial t = D\partial^2 c/\partial x^2$,

$$J_t = \frac{Dc_1}{L}\left[1 + 2\sum_{n=1}^{\infty}(-1)^n \exp\left(-\frac{Dn^2\pi^2 t}{L^2}\right)\right] \quad (2)$$

Integration of eqns. (1) and (2) from time zero to t, gives the relationship between the output pressure, $p_{H2,2}$ and time t in the form;

$$p_{H2,2} = \frac{ART_R\phi\sqrt{p_{H2,1}}}{V_2 L}\left[t - \frac{L^2}{6D} - \frac{2L^2}{D\pi^2}\sum_{n=1}^{\infty}\frac{(-1)^n}{n^2}\exp\left(-\frac{Dn^2\pi^2 t}{L^2}\right)\right] \quad (3)$$

where ϕ is the permeability of hydrogen and is equal to the product of the diffusivity D and the solubility constant K, so that

$$\phi = DK \quad (4)$$

K is defined by $c_1 = K\sqrt{p_{H2,1}}$, *i.e.* the Sieverts constant.

At longer times the exponential terms all become negligibly small, and the pressure becomes linear with time. The intercept, t_l, of this line on the time axis gives a determination of the diffusivity of hydrogen, *i.e.*

$$D = \frac{L^2}{6t_l} \quad (5)$$

This is the so-called "time-lag" method [16]. The permeability can also be determined from the slope of the straight line portion of the curve of eqn. (3). However, there was often uncertainty in the linearity between the pressure $p_{H2,2}$ and time t, especially for longer times, because the output pressure $p_{H2,2}$ was assumed to be negligibly low, such that $c_1 = K\sqrt{p_{H2,1}} \gg c_2 = K\sqrt{p_{H2,2}}$.

In the present investigation, in order to avoid this difficulty in the determination of the permeability, we used another analysis method based on the steady state permeation, which has been treated by Katz and Gulbransen [17]. In this case the flux is given as:

$$J_t = \frac{V_2}{ART_R}\frac{dp_{H2,2}}{dt} = \frac{\phi(\sqrt{p_{H2,1}} - \sqrt{p_{H2,2}})}{L} \quad (6)$$

By integrating for the steady state diffusion, one obtains

$$-\left[\ln\left(1 - \sqrt{\frac{p_{H2,2}}{p_{H2,1}}}\right) + \sqrt{\frac{p_{H2,2}}{p_{H2,1}}}\right] = \frac{ART_R\phi t}{2\sqrt{p_{H2,1}}V_2 L} \quad (7)$$

Thus, the permeability can be obtained from the slope of the straight line between $-[\ln(1-\sqrt{p_{H2,2}/p_{H2,1}})+\sqrt{p_{H2,2}/p_{H2,1}}]$ and time t.

Similar to the diffusivity D, the permeability ϕ is temperature dependent and is given in the form of the Arrhenius equation. Thus, the solubility constant K can be calculated from eqn. (4) as a similar Arrhenius type relation. In this report, the units of ϕ, D and K will be expressed as follows: $\phi=\phi_0 \exp(-Q_\phi/RT)$ ((mol H_2) m^{-1} s^{-1} $Pa^{-1/2}$), $D=D_0 \exp(-Q_D/RT)$ (m^2 s^{-1}) and $K=K_0 \exp(-Q_K/RT)$ ((mol H_2) m^{-3} $Pa^{-1/2}$), where $Q_\phi=Q_D+Q_K$ (J (mol H)$^{-1}$); Q_ϕ and Q_D are the activation energies for permeation and diffusion respectively, Q_K is the heat of solution, and $\phi_0=D_0K_0$; the pre-exponential factors respectively.

3. Results and discussion

3.1. Permeability

A typical example of the rise in output pressure with time is shown in Fig. 2, where the permeation transients are for alloys $Pd_{85-x}Y_xAg_{15}$ with $x=3.0$ and $Pd_{85-x}Gd_xAg_{15}$ with $x=3.0$ at a temperature of 673 K, and at various input pressures. The insets in the figures show enlarged versions of the plots at shorter times. The permeation rate increases with increasing input hydrogen pressure, and the higher the temperature, the more permeable the alloy. From the time intercept the diffusivity was calculated according

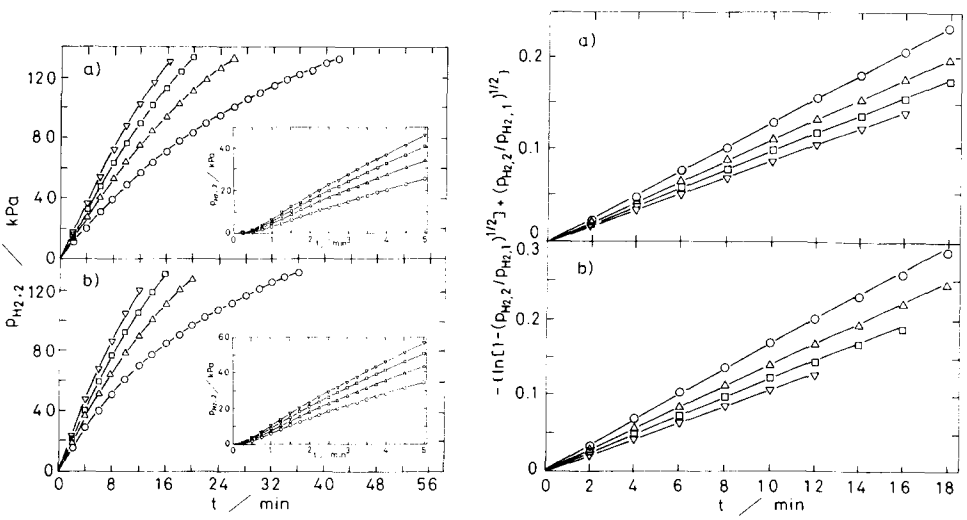

Fig. 2. Pressure build-up curves for hydrogen permeation through the alloys (a) $Pd_{85-x}Y_xAg_{15}$ with $x=3.0$ and (b) $Pd_{85-x}Gd_xAg_{15}$ with $x=3.0$ at 673 K and at various input hydrogen pressures: ○ 267 kPa, △ 400 kPa, □ 533 kPa, ▽ 667 kPa.

Fig. 3. $-\{\ln[1-(p_{H2,2}/p_{H2,1})^{1/2}]+(p_{H2,2}/p_{H2,1})^{1/2}\}$ *vs.* time for the alloys (a) $Pd_{85-x}Y_xAg_{15}$ with $x=3.0$ and (b) $Pd_{85-x}Gd_xAg_{15}$ with $x=3.0$ at 673 K and at various input hydrogen pressures: ○ 267 kPa, △ 400 kPa, □ 533 kPa, ▽ 667 kPa.

to eqn. (5). Figure 3 shows a plot of the left side of eqn. (7) *vs.* time for the same permeation data of Fig. 2. There is good linearity for the plots for the relatively high temperature experiments. However, in the cases of relatively low temperature experiments for much shorter times, the plots did not necessarily pass the origin because steady state permeation has not yet been established. However, since this problem does not influence the steady state permeability, the permeability of hydrogen in this study was calculated from the slopes of the straight lines over a range of relatively longer times.

An attempt was made to compare the permeability values ϕ in pure palladium obtained from the two analysis methods, one being the use of the slope of the straight line of eqn. (7), and the other the use of that of eqn. (3) for relatively shorter times. Table 1 shows a comparison between the permeability values calculated from the two analysis methods. It can be seen that the permeability values obtained from eqn. (7) at different temperatures and input pressures are generally slightly higher than those obtained from eqn. (3), and the former values are in good agreement with the previously reported values [18] within experimental error.

Figure 4 shows dependences of the permeability and diffusivity of hydrogen on the input hydrogen pressure in pure palladium and $Pd_{85-x}(Y(Gd))_xAg_{15}$ with $x=3.0$, as an example, at 573 K and 673 K. Although the ϕ and D values have a tendency to increase slightly with increasing input pressure at a given temperature, a significant pressure dependence was not observed in the input pressure and temperature ranges studied, *i.e.* 267–667 kPa, and 523–673 K. Thus, it can be seen that diffusion of hydrogen through the membranes is the rate-determining step in the permeation processes. So all the permeabilities and diffusivities of hydrogen reported here were obtained by averaging the values at different input pressures.

The temperature dependence of hydrogen permeability for a series of Pd–Y–Ag and Pd–Gd–Ag alloys is shown in Figs. 5 and 6, in comparison with those of pure palladium and some literature data [18]. The activation

TABLE 1

Comparison of the hydrogen permeability ϕ in pure palladium obtained from eqns. (3) and (7)

Analysis method	Input hydrogen pressure (kPa)	ϕ (10^{-9} (mol H_2) m^{-1} s^{-1} $Pa^{-1/2}$			
		523 K	573 K	623 K	673 K
Eqn. (3)	267	5.58	7.47	9.27	10.60
	400	6.07	7.08	9.51	10.87
	533	6.02	7.26	9.66	11.46
	667	6.93	7.47	9.83	11.71
Eqn. (7)	267	6.79	8.82	10.94	12.61
	400	7.25	8.39	11.09	12.63
	533	7.35	8.53	11.15	13.17
	667	8.02	8.65	11.18	13.43

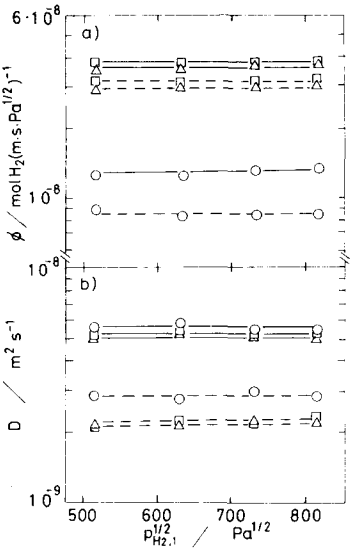

Fig. 4. Input hydrogen pressure dependences of (a) hydrogen permeability, and (b) diffusivity, in pure palladium (○), $Pd_{85-x}Y_xAg_{15}$ with $x=3.0$ (△) and $Pd_{85-x}Gd_xAg_{15}$ with $x=3.0$ (□) at ·—— 673 K and – – – 573 K.

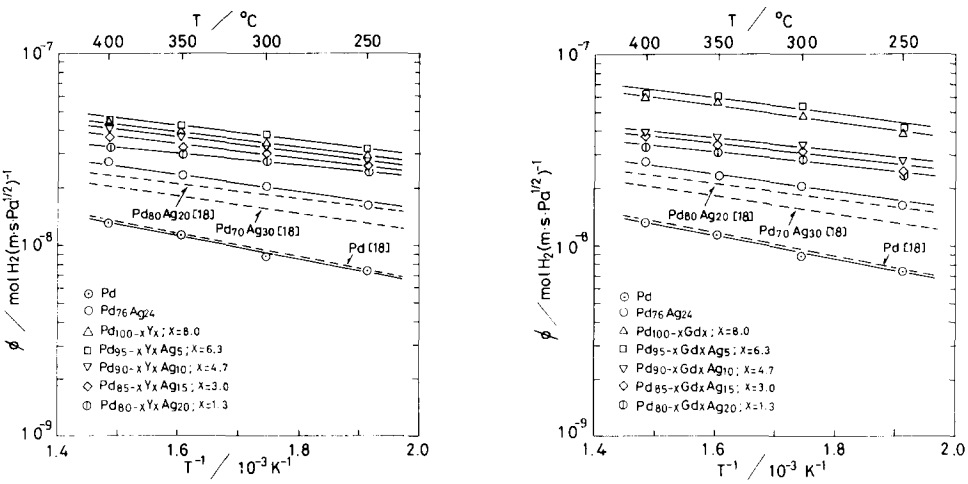

Fig. 5. Permeability of hydrogen in Pd–Y–Ag alloys *vs.* reciprocal temperature, together with that in pure palladium and literature data [18].

Fig. 6. Permeability of hydrogen in Pd–Gd–Ag alloys *vs.* reciprocal temperature, together with that in pure palladium and literature data [18].

energy for permeation Q_ϕ and the pre-exponential factor ϕ_0 for the alloys were obtained by a least-squares fit of log ϕ against $1/T$, and they are summarized in Table 2. The Q_ϕ and ϕ_0 values of pure palladium are in agreement with the results reported by Holleck [18], although Amano *et al.*

TABLE 2

Hydrogen permeabillity $\phi = \phi_0 \exp(-Q_\phi/RT)$, diffusivity $D = D_0 \exp(-Q_D/RT)$ and solubility constant $K = K_0 \exp(-Q_K/RT)$ in Pd–Y(Gd)–Ag alloys, together with that in pure palladium at temperatures between 523 K and 673 K, and input hydrogen pressures between 267 kPa and 667 kPa

Specimen	ϕ_0 (10^{-7} (mol H_2) m^{-1} s^{-1} $Pa^{-1/2}$)	Q_ϕ (10^3 J (mol H)$^{-1}$)	D_0 (10^{-7} m^2 s^{-1})	Q_D (10^4 J (mol H)$^{-1}$)	K_0 (10^{-1} (mol H_2) m^{-3} $Pa^{-1/2}$)	Q_K (10^4 J (mol H)$^{-1}$)
Pd	1.01	11.50±0.37	3.10	2.24±0.10	3.26	−1.09
$Pd_{100-x}Ag_x$ ($x=24.0$)	1.05	7.85±0.35	2.94	2.46±0.21	3.57	−1.68
$Pd_{100-x}Y_x$ ($x=8.0$)	1.84	8.01±0.21	2.14	2.31±0.16	8.60	−1.51
$Pd_{95-x}Y_xAg_5$ ($x=6.3$)	1.80	7.49±0.40	3.26	2.43±0.35	5.52	−1.68
$Pd_{90-x}Y_xAg_{10}$ ($x=4.7$)	1.66	7.77±0.37	6.44	2.80±0.30	2.58	−2.02
$Pd_{85-x}Y_xAg_{15}$ ($x=3.0$)	1.32	7.11±0.15	6.88	2.75±0.25	1.92	−2.04
$Pd_{80-x}Y_xAg_{20}$ ($x=1.3$)	0.90	5.74±0.14	5.91	2.63±0.22	1.52	−2.06
$Pd_{100-x}Gd_x$ ($x=8.0$)	2.17	7.27±0.29	5.90	2.58±0.24	3.68	−1.85
$Pd_{95-x}Gd_xAg_5$ ($x=6.3$)	2.27	7.19±0.45	8.00	2.63±0.35	2.84	−1.91
$Pd_{90-x}Gd_xAg_{10}$ ($x=4.7$)	1.26	6.47±0.33	8.68	3.02±0.45	1.45	−2.37
$Pd_{85-x}Gd_xAg_{15}$ ($x=3.0$)	1.26	6.61±0.40	10.30	2.92±0.32	1.22	−2.26
$Pd_{80-x}Gd_xAg_{20}$ ($x=1.3$)	1.00	6.21±0.28	5.92	2.66±0.22	1.69	−2.04

[19] obtained smaller values of Q_ϕ and ϕ_0 compared with the present results. The activation energy for permeation in the Pd–Y(Gd)–Ag alloys tends to decrease gradually with increasing silver content, and correspondingly with decreasing Y(Gd) content from that of the alloys $Pd_{100-x}(Y(Gd))_x$ with $x=8.0$, and shows a minor minimum around compositions of $Pd_{80-x}(Y(Gd))_xAg_{20}$ with $x=1.3$.

At the same temperature, the hydrogen permeabilities increase with an increase in Y(Gd) content and/or with a decrease in silver content from that of pure palladium, and at the same composition the permeabilities in the Pd–Gd–Ag alloys are slightly higher than those in the Pd–Y–Ag alloys. It was found that the alloys $Pd_{95-x}(Y(Gd))_xAg_5$ with $x=6.3$ are the most permeable to hydrogen, and the ϕ values in the alloys are about a factor of 2–2.5 higher than those in the Pd–24at.%Ag currently employed as commercial diffusion membranes. However, for practical applications, the former alloys may be difficult to make membranes out because of solid solution hardening, as examined previously [9].

Figure 7 shows a correlation between the hydrogen permeability at a temperature of 673 K, as an example, and the room temperature lattice parameter a_{ss} of hydrogen-free alloys determined previously [9], and Fig. 8 shows a relationship between the permeability and Vickers hardness [9]. It can be seen that the permeability increases with increasing lattice parameter and/or hardness from that of pure palladium, and thus the permeability is associated with the lattice expansion of the initial hydrogen-free alloys, which leads to the solid solution hardening.

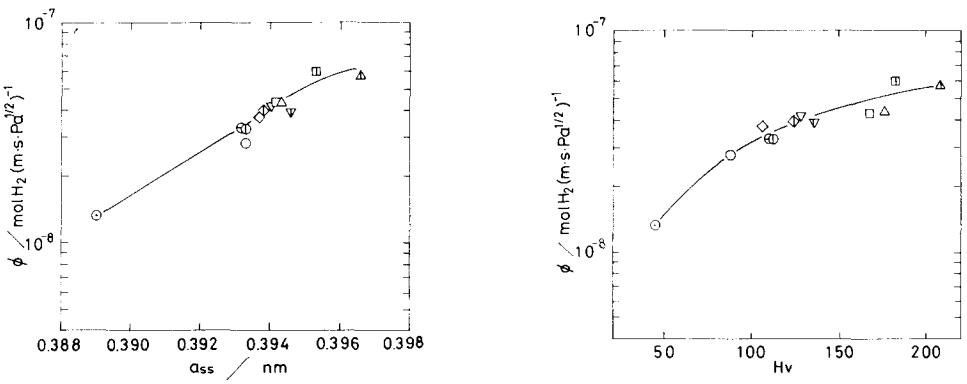

Fig. 7. Relationship between hydrogen permeability at 673 K in Pd–Y(Gd)–Ag alloys and room temperature lattice parameter of the hydrogen-free alloys [9]: ⊙ palladium; ○ $Pd_{76}Ag_{24}$; △ $Pd_{100-x}Y_x$, $x=8.0$; □ $Pd_{95-x}Y_xAg_5$, $x=6.3$; ▽ $Pd_{90-x}Y_xAg_{10}$, $x=4.7$; ◇ $Pd_{85-x}Y_xAg_{15}$, $x=3.0$; ⊕ $Pd_{80-x}Y_xAg_{20}$, $x=1.3$; ⧋ $Pd_{100-x}Gd_x$, $x=8.0$; ⧈ $Pd_{95-x}Gd_xAg_5$, $x=6.3$; ⧩ $Pd_{90-x}Gd_xAg_{10}$, $x=4.7$; ⧫ $Pd_{85-x}Gd_xAg_{15}$, $x=3.0$; ⊖ $Pd_{80-x}Gd_xAg_{20}$, $x=1.3$.

Fig. 8. Relationship between hydrogen permeability at 673 K in Pd–Y(Gd)–Ag alloys and Vickers hardness of the hydrogen-free alloys [9]: ⊙ palladium; ○ $Pd_{76}Ag_{24}$; △ $Pd_{100-x}Y_x$, $x=8.0$; □ $Pd_{95-x}Y_xAg_5$, $x=6.3$; ▽ $Pd_{90-x}Y_xAg_{10}$, $x=4.7$; ◇ $Pd_{85-x}Y_xAg_{15}$, $x=3.0$; ⊕ $Pd_{80-x}Y_xAg_{20}$, $x=1.3$; ⧋ $Pd_{100-x}Gd_x$, $x=8.0$; ⧈ $Pd_{95-x}Gd_xAg_5$, $x=6.3$; ⧩ $Pd_{90-x}Gd_xAg_{10}$; $x=4.7$; ⧫ $Pd_{85-x}Gd_xAg_{15}$, $x=3.0$; ⊖ $Pd_{80-x}Gd_xAg_{20}$, $x=1.3$.

As has been observed in previous studies [4, 9, 10], the alloys $Pd_{100-x}(Y(Gd))_x$ with $x=8.0$ and $Pd_{95-x}Gd_xAg_5$ with $x=6.3$ used in this study are more or less in short-range ordering of $Pd_7Y(Gd)$ and $Pd_7(Gd,Ag)$. It is known that the diffusivity of hydrogen in the ordered alloys is greater than that in the disordered state [2, 4, 20, 21], but the ordered alloys dissolve less hydrogen than do the disordered alloys [4, 22]. Therefore, the hydrogen permeability in Pd–8at.%Y(Gd) alloys and $Pd_{95-x}Gd_xAg_5$ with $x=6.3$ should be influenced by the short-range ordering of the alloys. In particular, the enhanced permeability in the $Pd_{95-x}Gd_xAg_5$ with $x=6.3$ seems to be attributable to the greater diffusivity due to the short-range order, as will be described later for hydrogen diffusivity and solubility.

However, as has been observed for Pd_3Mn alloys [23, 24], in order to examine the possibility of hydrogen-induced transitions of these alloys, the initially short-range ordered alloys of $Pd_{100-x}(Y(Gd))_x$ with $x=8.0$ and $Pd_{95-x}Gd_xAg_5$ with $x=6.3$ were exposed to hydrogen gas of $p_{H2}=667$ kPa at 673 K for 10 h, cooled to room temperature with the pressure being maintained, and were then examined by electron diffraction. Transitions of order to disorder were slightly observed for these alloys.

Furthermore, an attempt was made to compare the hydrogen permeabilities through pure palladium, Pd–24at.%Ag and $Pd_{100-x}(Y(Gd))_x$ with $x=8.0$ obtained in the present study with previously reported results [2]. In the previous work of Hughes and Harris [2], they defined the permeability as $J=DA\Delta c/L$ (m^3 (NTP) m^{-2} s^{-1}) for a convenient expression, *i.e.* corresponding to eqn. (6) in the present paper, where Δc is the difference in hydrogen concentration between the input and output pressures. In order to compare the data, the input pressure of $p_{H2,1}=667$ kPa in this study was selected, although the pressure in the previous study [2] was $p_{H2,1}=689$ kPa, and the sample thickness was normalized to $L=1\times10^{-4}$ m, *i.e.* the same thickness, by assuming that the output pressure rise with time, $d_{pH2,2}/dt$, is inversely

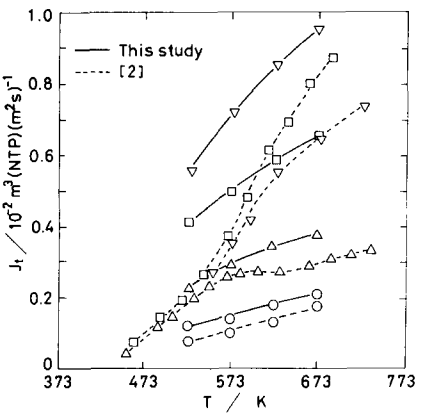

Fig. 9. Comparison of the present hydrogen permeability in pure palladium, Pd–24at.%Ag and $Pd_{100-x}(Y(Gd))_x$ with $x=8.0$, and literature data [2]: ○ pure palladium, △ Pd–24at.%Ag, literature data Pd–25at.%Ag, □ $Pd_{100-x}Y_x$ with $x=8.0$, ▽ $Pd_{100-x}Gd_x$ with $x=8.0$.

proportional to the sample thickness. Figure 9 shows a comparison of permeability with temperature from the literature [2] and obtained in the present study. The present hydrogen permeabilities in pure palladium, Pd–24at.%Ag and $Pd_{100-x}(Y(Gd))_x$ with $x = 8.0$ are generally larger than those of the previous studies [2] over a wide range of temperatures, except for the permeability of the alloys $Pd_{100-x}Y_x$ with $x = 8.0$ at higher temperatures. Furthermore, the present results for alloys $Pd_{100-x}(Y(Gd))_x$ with $x = 8.0$ are in disagreement with those of Hughes and Harris [2] who reported that the alloy $Pd_{100-x}Y_x$ with $x = 8.0$ exhibited higher permeabilities than the alloy $Pd_{100-x}Gd_x$ with $x = 8.0$ at all temperatures and input pressures.

In the hydrogen permeation transients, the uphill effects associated with self-strain gradient-induced diffusion of hydrogen interstitials [25, 26] in the alloy membranes were not observed, because the samples were in the initial hydrogen-free state.

3.2. Diffusivity

Figures 10 and 11 show the temperature dependence of hydrogen diffusivity for a series of Pd–Y–Ag and Pd–Gd–Ag alloys, in comparison with those of pure palladium and some literature data [2, 18]. The diffusivity values for Pd–8at.%Y(Gd), Pd–5.75at.%Ce and Pd–25at.%Ag alloys reported by Hughes and Harris [2] are located in the region between the two dotted lines in the figures. The activation energy for diffusion Q_D and the pre-exponential factor D_0 for the alloys were obtained by a least-squares fit of the Arrhenius plots, and they are also given in Table 2.

As can be seen from Figs. 10 and 11, the diffusivity values in the present pure palladium are in good agreement with the previously reported results

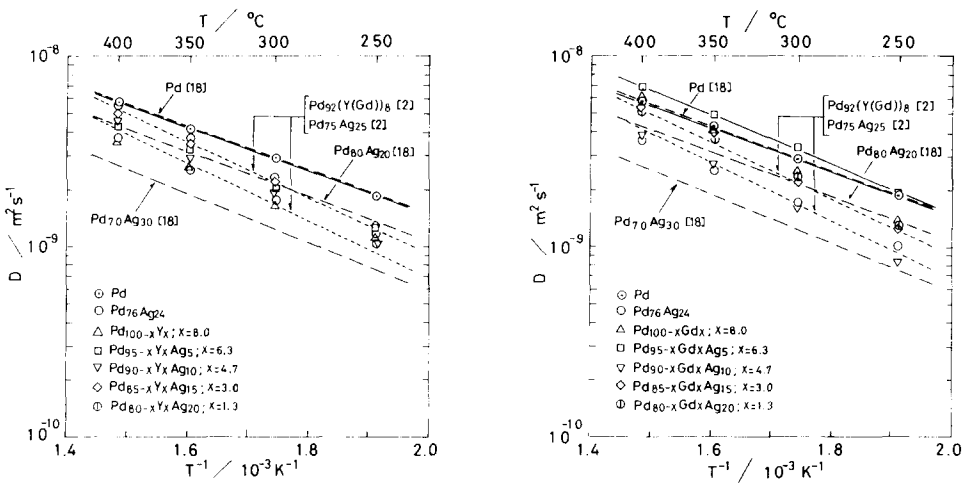

Fig. 10. Diffusivity of hydrogen in Pd–Y–Ag alloys *vs.* reciprocal temperature, together with that in pure palladium and literature data [2, 18].

Fig. 11. Diffusivity of hydrogen in Pd–Gd–Ag alloys *vs.* reciprocal temperature, together with that in pure palladium and literature data [2, 18].

[18, 19, 27]. The D values at the same temperature in the Pd–Y(Gd)–Ag alloys tend to decrease with increasing solute metal contents of silver and/or Y(Gd), from that of pure palladium, except for the alloy $Pd_{95-x}Gd_xAg_5$ with $x = 6.3$, where the alloy exhibits higher diffusivities than those of pure palladium. The present diffusivity values in the alloys $Pd_{100-x-y}(Y(Gd))_xAg_y$ where $y = 0$–24at.%Ag and $x = 1.3$–8.0at.%Y(Gd) are in reasonable agreement with the previous data of Pd–8at.%Y(Gd) and Pd–25at.%Ag alloys reported by Hughes and Harris [2], who showed that the values of Q_D and D_0 for these alloys are almost the same within experimental error. However, the activation energies Q_D for diffusion in the present study tend to increase gradually with increasing silver content and/or decreasing Y(Gd) content, and the energy values exhibit a minor maximum around compositions with 10–15at.%Ag and 3.0–4.7at.%Y(Gd).

Comparison of the previous diffusivity data in Pd–8.0at.%Y alloy determined for the temperature range 280–333 K by an electrochemical method [20] shows that if the present data are extrapolated to lower temperatures, *i.e.* room temperature, the diffusivity values are in reasonable agreement with the previous data [20], although the pre-exponential factor D_0 and the activation energy for diffusion Q_D are slightly lower than those of the present high temperature data. This discrepancy in the D_0 and Q_D values may be due to measurements over a limited narrow temperature range [20].

3.3. Solubility constant

Combining the above values of ϕ and D using eqn. (4), the hydrogen solubility constants K, *i.e.* the solubilities per unit square root of input pressure, were calculated. The temperature dependences of the solubility constants in the Pd–Y–Ag and Pd–Gd–Ag alloys are shown in Figs. 12 and 13 respectively. The heat of solution of hydrogen Q_K and the pre-exponential factor K_0 are also summarized in Table 2.

The heat of solution and the pre-exponential factor, *i.e.* the entropy term in the present pure palladium is in agreement with the previously reported result [18]. The Q_K values in the Pd–Y(Gd)–Ag alloys tend to increase in exothermicity with increasing silver content and/or with decreasing Y(Gd) content, and the heats of solution in exothermicity exhibit a minor maximum near compositions of 15at.%Ag and 3.0at.%Y(Gd). The solubility constants at the same temperature in Pd–Y(Gd)–Ag alloys are much greater than those in pure palladium; in particular, the alloys with higher Y(Gd) and lower silver contents dissolve more hydrogen. The dependence of hydrogen solubility on alloy composition is consistent with hydrogen solubility data for Pd–Ag [28], Pd–Y [29] and Pd–Gd [30] alloys.

Therefore, it can be seen that the enhancement of hydrogen permeability in Pd–Y(Gd)–Ag alloys with high Y(Gd) content is generally due to both the higher hydrogen solubility gradients and diffusivities. Judging from the hardness measurements carried out previously [9], the alloys $Pd_{100-x-y}(Y(Gd))_xAg_y$ with compositions where y is about 15–20at.%Ag, and the corresponding x values of yttrium and/or gadolinium are 1.3–3.0at.%, seem to be better

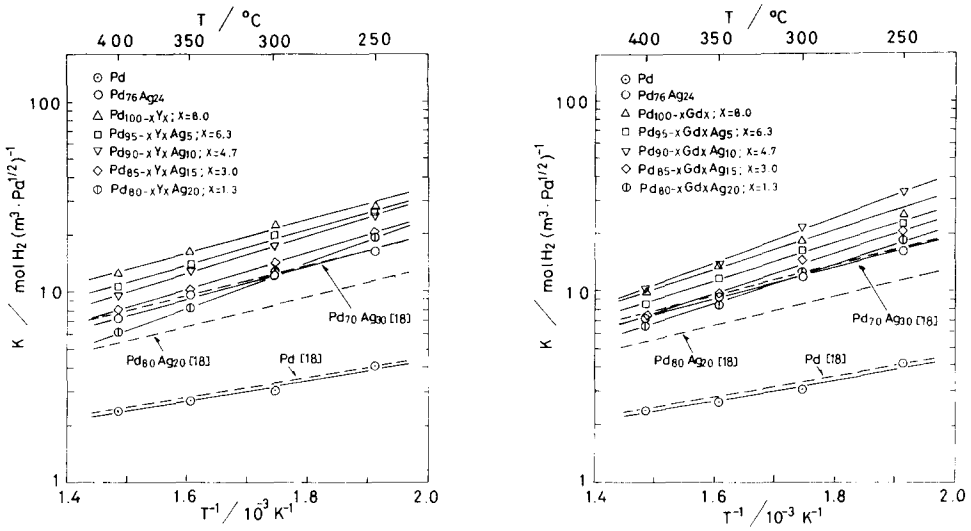

Fig. 12. Solubility constant of hydrogen in Pd–Y–Ag alloys *vs.* reciprocal temperature, together with that in pure palladium and literature data [18].

Fig. 13. Solubility constant of hydrogen in Pd–Gd–Ag alloys *vs.* reciprocal temperature, together with that in pure palladium and literature data [18].

materials for hydrogen diffusion membranes than the Pd–(23–25)at.%Ag employed commercially or the Pd–8at.%Y alloys proposed by Hughes and Harris [2]; they have greater hydrogen permeability and form stronger membranes than the Pd–(23–25)at.%Ag, and form softer membranes than the Pd–8at.%Y(Gd).

4. Conclusions

(1) The dependence of the permeability and solubility on input hydrogen pressure in Pd–Y(Gd)–Ag alloys and pure palladium is not significant in the pressure and temperature ranges studied.

(2) The hydrogen permeabilities in Pd–Y(Gd)–Ag alloys at the same temperature increase with increasing Y(Gd) content and/or with decreasing silver content from that of pure palladium, and the alloys $Pd_{95-x}(Y(Gd))_xAg_5$ with $x = 6.3$ exhibit greater permeabilities than $Pd_{100-x}(Y(Gd))_x$ with $x = 8.0$. At the same composition, the permeabilities in the Pd–Gd–Ag alloys are slightly higher than those in the Pd–Y–Ag alloys. The hydrogen permeabilities increase with increasing lattice parameter of the initial hydrogen-free alloys, although the lattice expansion leads to solid solution hardening.

(3) The diffusivity of hydrogen in Pd–Y(Gd)–Ag alloys at the same temperature decreases with increasing the solute metal content of silver and/or Y(Gd) from that of pure palladium, except for the alloy $Pd_{95-x}Gd_xAg_5$ with $x = 6.3$, where the alloy exhibits a higher diffusivity than pure palladium.

(4) The hydrogen solubility constants in Pd–Y(Gd)–Ag alloys at the same temperature are much greater than those in pure palladium; in particular, the alloys with higher Y(Gd) and lower silver contents dissolve more hydrogen.

(5) The enhancement of hydrogen permeabilities in the Pd–Y(Gd)–Ag alloys with high Y(Gd) content is generally due to both the higher hydrogen solubility gradients and diffusivities. Judging from the results of hardness measurements, the alloys $Pd_{100-x-y}(Y(Gd))_xAg_y$ with compositions where y is about 15–20 at.% Ag, and the corresponding x values of yttrium and/or gadolinium contents are 1.3–3.0 at.%, seem to be better materials for hydrogen diffusion membranes than Pd–(23–25)at.%Ag alloys.

Acknowledgments

The authors would like to express their gratitude to Tanaka Kikinzoku Kogyo K. K. for the loan of the palladium metal.

References

1 D. Fort, J. P. G. Farr and I. R. Harris, *J. Less-Common Met.*, *39* (1975) 293.
2 D. T. Hughes and I. R. Harris, *J. Less-Common Met.*, *61* (1978) 9.
Z. Phys. Chem. N.F., *117* (1979) 185.
3 D. T. Hughes, J. Evans and I. R. Harris, *J. Less-Common Met.*, *74* (1980) 255.
4 M. L. Doyle and I. R. Harris, *Platinum Met. Rev.*, *32* (1988) 130.
5 F. A. Lewis, *The Palladium–Hydrogen System*, Academic Press, New York, 1967.
6 A. G. Knapton, *Platinum Met. Rev.*, *21* (1977) 44.
7 M. L. H. Wise, J. P. G. Farr and I. R. Harris, *J. Less-Common Met.*, *41* (1975) 115.
8 Y. Sakamoto, K. Yuwasa and K. Hirayama, *J. Less-Common Met.*,*88* (1982) 115.
9 Y. Sakamoto, F. L. Chen, M. Furukawa and K. Mine, *J. Less-Common Met.*, *166* (1990) 45.
10 Y. Sakamoto, K. Takao, M. Yoshida and T. B. Flanagan, *J. Less-Common Met.*, *143* (1988) 207.
K. Takao, Y. Sakamoto, M. Yoshida and T. B. Flanagan, *J. Less-Common Met.*, *152* (1989) 115.
11 Y. Sakamoto, F. L. Chen, M. Furukawa and K. Mine, *J. Less-Common Met.*, *159* (1990) 191.
12 F. L. Chen, M. Furukawa and Y. Sakamoto, *J. Less-Common Met.*, *155* (1989) 173.
13 W. A. Rogers, R. S. Buritz and D. Alpert, *J. Appl. Phys.*, *25* (1954) 868.
14 W. M. Robertson, *Z. Metallkde.*, *64* (1973) 436.
15 J. Crank, *The Mathematics of Diffusion*, Clarendon Press, Oxford, 1955, p. 45.
16 R. M. Barrer, *Trans. Faraday Soc.*, *35* (1939) 628.
17 O. M. Katz and E. A. Gulbransen, *Rev. Sci. Instrum.*, *31* (1960) 615.
18 G. L. Holleck, *J. Phys. Chem.*, *74* (1970) 503.
19 M. Amano, C. Nishimura and M. Komaki, *Mater. Trans. JIM.*, *31* (1990) 404.
20 Y. Sakamoto, H. Kaneko, T. Tsukahara and S. Hirata, *Scripta Metall.*, *21* (1987) 415.
21 Y. Sakamoto and Y. Tanaka, *Rep. Fac. Eng., Nagasaki Univ.*, *17* (28) (1987) 49.
22 Y. Sakamoto, T. B. Flanagan and T. Kuji, *Z. Phys. Chem. N. F.*, *143* (1985) 61.
23 T. B. Flanagan, A. P. Craft, T. Kuji, K. Baba and Y. Sakamoto, *Scripta Metall.*, *20* (1986) 1745.
24 K. Baba, Y. Sakamoto, T. B. Flanagan and A. P. Craft, *Scripta Metall.*, *21* (1987) 299.

25 F. A. Lewis, J. P. Magennis, S. G. McKee and P. J. M. Ssebuwufu, *Nature, 306* (1983) 673.
26 F. A. Lewis, K. Kandasamy and B. Baranowski, *Platinum Met. Rev., 32* (1988) 22.
27 J. Völkl and G. Alefeld (ed.), *Topics in Applied Physics, Hydrogen in Metals I*, Springer, Berlin, 1978, p. 321.
28 H. Brodowsky and E. Poeschel, *Z. Phys. Chem. N. F., 44* (1965) 143.
29 Y. Sakamoto, K. Kajihara, Y. Fukusaki and T. B. Flanagan, *Z. Phys. Chem. N. F., 159* (1988) 61.
30 Y. Sakamoto, F. L. Chen, M. Furukawa and T. B. Flanagan, *Ber. Bunsenges. Phys. Chem., 94* (1990) 190.